ACS APPLIED MATERIALS & INTERFACES

Research Article

www.acsami.org

Random Networks of Single-Walled Carbon Nanotubes Promote Mesenchymal Stem Cell's Proliferation and Differentiation

Jae-Hyeok Lee,[†,⊥] Wooyoung Shim,[†,⊥] Najeeb Choolakadavil Khalid,[†,§] Won-Seok Kang,[†] Minsu Lee,[†] Hyo-Sop Kim,[†] Je Choi,[†] Gwang Lee,*[,‡] and Jae-Ho Kim*[,†]

[†]Department of Molecular Science and Technology, Ajou University, Suwon 443-749, Republic of Korea

[‡]Department of Physiology, Ajou University School of Medicine, Suwon 443-721, Republic of Korea

Supporting Information

ABSTRACT: Studies on the interaction of cells with single-walled carbon nanotubes (SWCNTs) have been receiving increasing attention owing to their potential for various cellular applications. In this report, we investigated the interactions between biological cells and nanostructured SWCNTs films and focused on how morphological structures of SWCNT films affected cellular behavior such as cell proliferation and differentiation. One directionally aligned SWCNT Langmuir–Blodgett (LB) film and random network SWCNT film were fabricated by LB and vacuum filteration methods, respectively. We demonstrate that our SWCNT LB and network film based scaffolds do not show any cytotoxicity, while on the other hand, these scaffolds promote differentiation property of rat mesenchymal stem cells (rMSCs) when compared with that on conventional tissue culture polystyrene substrates. Especially, the SWCNT network film with average thickness and roughness values of 95 ± 5 and 9.81 nm, respectively, demonstrated faster growth rate and higher cell thickness for rMSCs. These results suggest that systematic manipulation of the thickness, roughness, and directional alignment of SWCNT films would provide the convenient strategy for controlling the growth and maintenance of the differentiation property of stem cells. The SWCNT film could be an alternative culture substrate for various stem cells, which often require close control of the growth and differentiation properties.

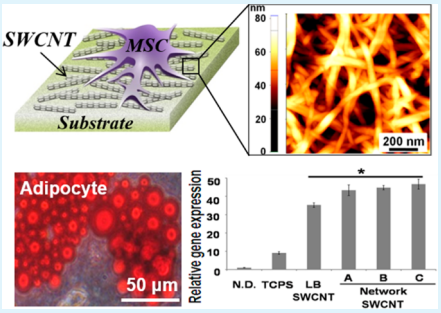

KEYWORDS: *carbon nanotube, Langmuir–Blodgett films, mesenchymal stem cell, growth pattern, differentiation, promote*

1. INTRODUCTION

Self-renewable and multipotent characteristics of mesenchymal stem cells (MSCs) have demonstrated great potential for a breakthrough in limits of the modern medicine.[1−3] MSCs can also trans-differentiate into specific tissue cells, such as osteoblasts,[4] chondrocytes,[5] adipocytes,[6] and even to neuronal cells[7] both in vitro and in vivo. Unlike embryonic stem cells, MSCs are possible to isolate from a variety of tissues, including bone marrow,[8] adipose tissues,[6,9] and umbilical cord blood.[10] In addition, use of these cells is easier due to less argument in ethical issues in the stem cell research and further application in medicine.[11] Because MSCs are undifferentiated stem cells, their properties are susceptible to change by internal and external stimuli. Therefore, ex vivo culture expansion and preservation of inherent properties of the stem cell became critical issues for further development of the stem cell researches. Recently, control of cell adhesion and growth on nanostructured surfaces, especially on carbon nanotube (CNT) surfaces, has been receiving great attention owing to its potential for various cellular applications.

Since their discovery in 1991,[12] CNTs have attracted much attention not only for their unique electrical and mechanical properties but also for a wide variety of biological applications, such as tissue engineering scaffolds,[13] delivery of drugs,[14] cell tracking,[15] and growth platform for neuronal circuits.[16−18] In addition, several studies have reported the interaction between CNTs and various cells such as mammalian cells,[19−21] stem cells,[16,22−24] and neural cell,[25,26] including alignment of those cells on CNT patterns.[27] In particular, Mattson et al. showed for the first time that neurons grew well on multi-walled carbon nanotubes (MWCNTs)-based substrate for in vitro growth of embryonic rat hippocampal neurons.[28] Firkowska et al. demonstrated human osteoblast cell responses to nanoscaled topography of MWCNT-based matrices with excellent spreading and metabolic activity.[29] Firkowska et al. found that the osteoblast cells on glass have the lowest cell stiffness compared with cells adhered to a MWCNT surface. Furthermore, they suggested regular topography of MWCNT-based matrices, which included the presence of tight junctions and a high-quality adhesion with each other leading to a good biocompatibility with the cell. Several other studies also have been explored to demonstrate the interactions of CNTs with various cells.[30] However, there are only a few studies reported on the effect of nanometer scale variation of scaffold on the

Received: October 5, 2014
Accepted: December 29, 2014
Published: December 29, 2014

DOI: 10.1021/am506833q
ACS Appl. Mater. Interfaces 2015, 7, 1560−1567

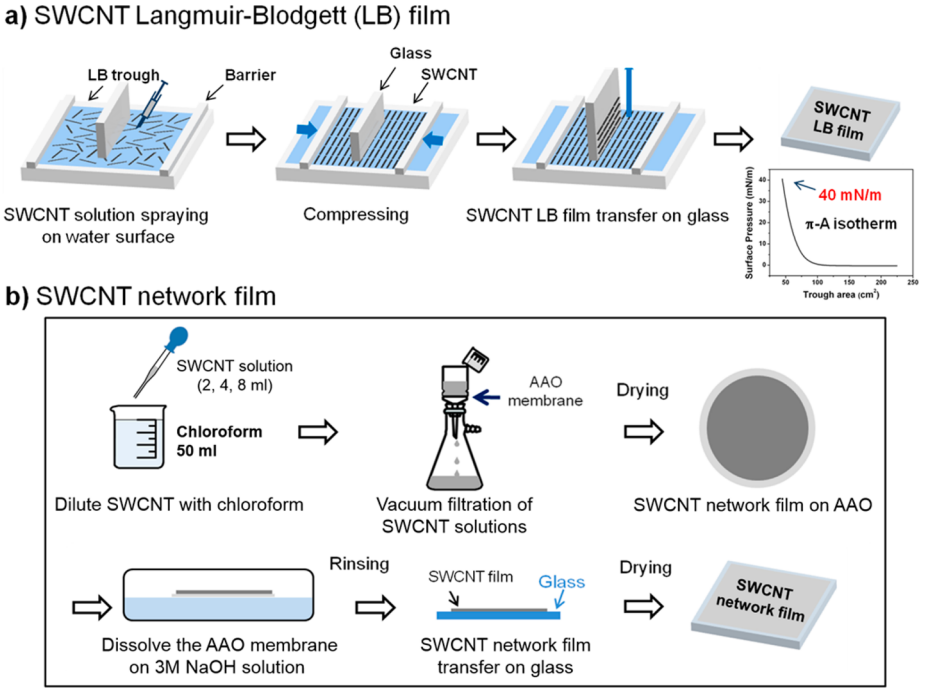

Figure 1. (a, b) Schematic diagram of fabrications of SWCNT LB film and network films by LB and filtration method, respectively.

morphology and differentiation of MSCs. The aim of this study is to systematically investigate how the growth and differentiation properties of MSCs cultured on various single-walled carbon nanotube (SWCNT) films are affected by the control of film thickness and surface roughness in the nanometer scale. Highly oriented SWCNT Langmuir–Blodgett (LB) films and random network SWCNT films with various thicknesses and roughness were used as culture substrates to investigate the growth pattern and differentiation of rat MSCs (rMSCs) on SWCNT films. The morphology, viability and differentiation property of rMSCs on these SWCNTs films were examined by using atomic force microscopy (AFM), MTT assay, and adipogenesis, respectively. Our study provides fundamental information on biocompatibility and means of enhancing the cell growth and differentiation with SWCNT substrate. Furthermore, our study demonstrates the possibility of utilizing the SWCNT substrates as a potential culture scaffolds for the precise control of growth and differentiation of the MSCs.

2. EXPERIMENTAL SECTION

2.1. Chemicals and Materials. SWCNTs synthesized by the arc discharge method were purchased from Iljin Nanotech Co. (Seoul, Korea). We used thiophenyl-modified SWCNT (SWCNT-SHs) solution for fabricating SWCNT LB film and network SWCNT film on 1 mm thick glass substrates (26 × 26 mm, Marienfeld, Germany). The SWCNT-SHs solution in chloroform was prepared according to the process described in our previous reports.[32] In a typical experiment, purified SWCNTs were shortened and carboxylated by chemical oxidation in a mixture of concentrated sulfuric and nitric acids (3:1, v/v, 98% and 70%, respectively) under ultrasonic agitation (Cole-Palmer, 55 kHz) at 70 °C for 4 h. The reaction mixture was filtered through an alumina filter (Anodisk, Whatman Inc., USA, pore size = 0.2 μm). The remains left on the filter were then washed with deionized water until the filtrate pH became nearly neutral. The resulting filtrate was dispersed by ultrasonication for 1 h in an aqueous Triton X-100 surfactantsolution (250 mL, 3 wt %). Immediately after sonication, the sample was centrifuged at 6000 rpm for 1 h. The supernatant was carefully decanted. The resulting carboxyl functionalized SWCNT suspension was then treated with 4-aminothiophenol in the presence of 1-[2-(dimethylamino)propyl]-3-ethylcarbodiimide hydrochloride (EDC) and *N*-hydroxysuccinimide (NHS) to make SWCNT-SHs solution. The functionalized SWCNTs obtained were dissolved in chloroform by ultrasonication.

2.2. Preparation of SWCNT LB Film and Network SWCNT Film. Thin films of SWCNTs were prepared on glass substrates by the LB method and vacuum filtration method. Figure 1a shows schematic illustration of the prepration of SWCNT LB flms via LB technique, and a prepration of network SWCNT films through filter method is also shown (Figure 1b).

Langmuir–Blodgett Method. The glass substrates were submerged into water in the LB trough (KSV 10002, KSV instruments, Finland). The SWCNT-SHs solution in $CHCl_3$ was spread on the air/water interface by carefully dropping minute droplets of SWCNTs solution up to a total volume of 4 mL. After the solvent was evaporated, the SWCNT bundles remained on the air/water interface. Then, it was compressed by moving the barriers at a speed of 4 mm/min until the surface pressure reached 40 mN/m. A vertical dipping method was employed to transfer the SWCNTs from the air/water interface onto the glass substrates with a lifting speed of 1 mm/min while maintaining the surface pressure of 40 mN/m. The SWCNT LB films were annealed at 120 °C for 3 h under nitrogen atmosphere.

Vacuum Filtration Method. SWCNT-SHs solution (2, 4, and 8 mL, 30 mg/L in $CHCl_3$) was filtered through an anodic aluminum oxide filter membrane with a pore size of 0.2 μm and an effective area of 11.3 cm^2. The resulting thin film of SWCNTs on the alumina filter was carefully placed on 3 M aqueous sodium hydroxide (NaOH) solution. When the alumina filter was completely dissolved in NaOH solution, a thin film of the network SWCNT sample was remained on the surface. The NaOH solution was drained off using an aspirator and carefully washed the film several times with distilled water until the pH reached nearly 7. The film was then transferred from the water surface to the glass substrate by slowly removing the water using an aspirator. The films were annealed at 120 °C for 3 h under nitrogen atmosphere.

2.3. Isolation and Culture of Rat Bone Marrow Mesenchymal Stem Cells. Bone marrow aspirates (10 mL) were obtained from adult Sprague-Dawley rats (Samtako, Korea), weighing 300–320 g, which were housed under environmentally controlled conditions at 23 ± 2 °C and 50 ± 10% humidity and given free access to food and water. The femurs were isolated from the rats, and both ends of the

DOI: 10.1021/am506833q
ACS Appl. Mater. Interfaces 2015, 7, 1560–1567

femurs were removed. The remaining bones were centrifuged at 1500 rpm for 20 min. To eliminate red blood cells, the supernatant was discarded, and the cell pellets were washed with PBS. After red blood cells were eliminated from bone marrow aspirates, the rMSCs were cultured in low-glucose Culbecco modified Eagle's media (LG-DMEM, Gibco, USA) at 37 °C in humidified atmosphere of 5% CO_2, and were supplemented with heat-inactivated 10% fetal bovine serum (Gbco, USA), 50 units/ml penicillin, and 0.05 mg/mL streptomycin (Gibco, USA). Two days later, nonadherent cells were removed by replacing the medium (passage 0). On the seventh day of incubation, the cells were trypsinized with 0.25% trypsin/0.1% EDTA (Sigma) and replaced on culture dishes (passage 1). The passage 4 rMSCs were cultured on four kinds of SWCNT films including LB film, and network films with different thicknesses prepared by filtering 2, 4, and 8 mL SWCNT-SHs solution.

2.4. MTT Cytotoxicity Assay. After 72 h of incubation in SWCNT films, cell viability assay was performed using MTT ((3-(4,5-dimethylthiazol-2-yl)-2,5-diphenyltetrazolium bromide), Promega, USA). The rMSCs were cultured at a density of 5×10^5 cells per plate containing SWCNT film for 72 h. After that, culture media were removed, and fresh medium containing 2 mg/mL MTT was placed for 30 min at 37 °C, and the optical densities of each well were measured using an automated plate reader (Biotech Instruments, USA) at 490 nm. Absorbance values were averaged triplicate measurement of samples, and standardized using triplicate blank and control values.

2.5. Adipogenesis of rMSC. Adipogenic differentiation was induced in passage 4 rMSC (3.15×10^4 cell/cm^2) plating in TCPS and SWCNT films, and incubated at 37 °C in humidified atmosphere of 5% CO_2 for 24 h before induction of adipogenic differentiation. When the cells reached 80% confluency, we removed nonreached cells and replaced with adipogenic differentiation medium (PromoCell, Heidelberg, Germany) supplemented with 10% FBS (Gibco, CA, USA), 50 units/mL penicillin, and 0.05 mg/mL streptomycin (Gibco, CA, USA), and cells were incubated at 37 °C in humidified atmosphere of 5% CO_2. To maintain the cells in an adipogenic differentiation, medium was changed every 72 h for 15 days. The adipogenic differentiation was confirmed by Oil Red O staining (the details are described below).

2.6. Oil Red O Staining. To assess adipogenic differentiation of rMSCs in SWCNT films, Oil Red O staining was performed after 10 days of culture in adipogenic differentiation medium. Briefly, cells were fixed in 4% formaldehyde solution for 10 min, and then rinsed with 10× phosphate buffered saline (PBS) three times. The Oil Red O (Sigma, MO, USA), which is dissolved in 60% isopropyl alcohol, was added into cells, and the mixture was incubated at room temperature for 20 min. The cells were washed with distilled water three times, and Oil Red O stained cells were captured using light microscopy (Nikon Cxlipse TE300; Olympus, Tokyo, Japan).

2.7. RNA Purification and Semiquantitative Reverse Transcription PCR. RNA was isolated from differentiated or non-differentiated rMSCs using RNA isolation reagent (RNA Bee, Tel-Test, Inc., USA) according to the manufacturer's instructions. Briefly, cells were harvested and treated with RNAzol B (500 μL). Chloroform was then added and the mixture was incubated at 4 °C for 5 min. Total RNA was precipitated with isopropyl alcohol (200 μL), and RNA pellets were washed with 70% ethanol. RNA was eluted from pellets using RNase-free water (WelGene, Korea) and quantified by spectrophotometry (Eppendorf, USA). To quantify expression of differentiation marker genes, total RNA samples were reverse-transcribed using the ImProm-II Reverse Transcription system (Promega, USA), according to the manufacturer's instructions, and then amplified using gene-specific primer pairs; peroxisome proliferator-activated receptor γ (PPARγ forward: GCTGTTATG GGTGAAACTCTG, reverse: ATAAGGTGGAGATGCAGGCTC), adipsin (forward: GGTCACCCAAGCAACAAAGT,reverse: CCTCCTGCCTTCAAGTCATC), and glyceraldehyde-3-phosphate dehydrogenase (GAPDH, forward: CATGACCAC AGTCCATGCCATCACT, reverse: TGAGGTCCACCACCCTGTTGCTGTA). Amplified PCR product quantities were calculated and normalized using Multi Gauge 3.0 software (Fujifilm, Japan). PCR reactions were run in triplicate, and normalized versus GAPDH PCR products were amplified from the same samples to remove template error.

2.8. Instrumentation for Characterization. For the analysis of SWCNT LB film and network films, we used scanning electron microscopy (SEM, LEO SUPRA 55, Carl Zeiss NTS GmgH) operating at 10 kV. All AFM images were recorded on a XE-100 AFM system (Park Systems Corp., Korea) in noncontact mode under constant temperature and humidity conditions. TETRA 15 noncontact cantilevers (M2N, Inc., Korea) were used to fabricate SWCNT capped tip for high resolution AFM image measurement. A detailed fabrication procedure for SWCNT capped tip was described elsewhere.[31] AFM images were measured by utilizing the prepared SWCNT capped tip with a resonance frequency of approximately 300−310 kHz. The ζ-potentials of bare glass, SWCNT films, and SWCNT-SHs suspension solution were measured by a ζ-potential analyzer (ELSZ-2, Otsuka Electronics Korea Co., Ltd.). The room-temperature (24 °C) static contact angle of deionized water (droplet of 3 μL) on the bare glass and SWCNT films was obtained by a contact angle analyzer (Phoenix 150, SEO) using a sessile drop method.

3. RESULTS AND DISCUSSION

In this study, we used a stable dispersion of thiophenyl-modified SWCNTs in chloroform (0.3 mg/L), which consisted

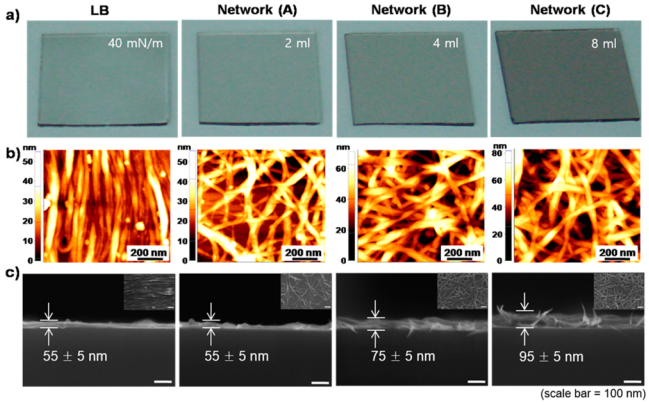

Figure 2. (a, b) Optical microscopic and AFM images of the bare glass, SWCNT LB and network films. (c) SEM images of cross-sectioned SWCNT films with different thicknesses fabricated by the LB and filtration methods. Network films (A), (B), and (C) were prepared with 2, 4, and 8 mL of the suspension of SWCNT, respectively. Scale bars in SEM images including top-view images of the films in the inset in panel c correspond to 100 nm.

Table 1. Thickness, Average Roughness, Transmittance and Resistance of SWCNT Films and Bare Glass

		network			
parameters	bare glass	LB	(A)	(B)	(C)
thickness (nm)[a]		55 ± 5	55 ± 5	75 ± 5	95 ± 5
roughness (nm)[a]	0.17	5.81	6.62	9.22	9.81
transmittance (%)	100	87.2	89.9	82.4	69.8

[a]Values represent average of 5 measurements.

of uniform sized SWCNT bundles with an average diameter and length of 50 ± 10 nm and 1.5 ± 0.2 μm, respectively (Figure S1, Supporting Information). Hierarchically aligned SWCNT LB films were constructed by using the LB technique. As described in our previous report, we demonstrated that compression of SWCNTs on a LB trough led to formation of uniform and stable SWCNT Langmuir films, where the SWCNTs were hierarchically aligned parallel to the trough

DOI: 10.1021/am506833q
ACS Appl. Mater. Interfaces 2015, 7, 1560−1567

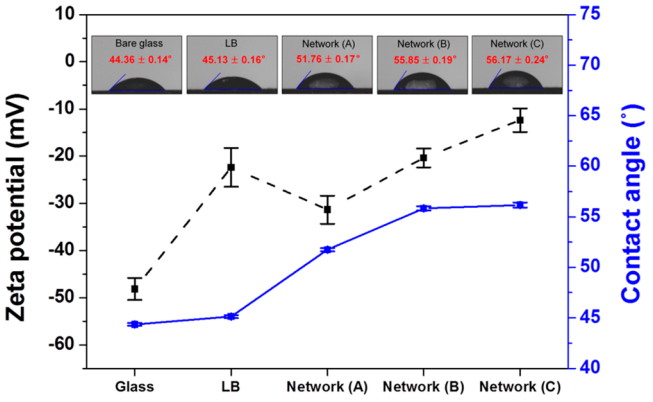

Figure 3. ζ-Potential and contact angle measurements data of the bare glass and four different SWCNT films.

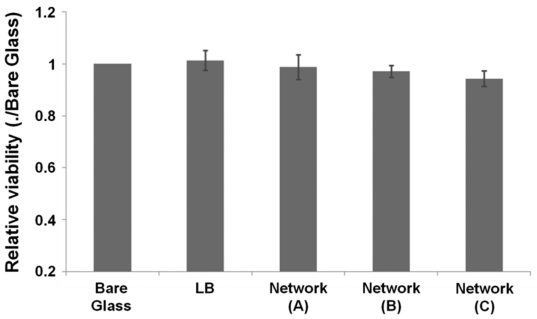

Figure 5. Relative viability of rMSCs cultured on a bare glass as a control and four different SWCNT films for 3 days, which is measured by MTT assay.

barriers.[32] The SWCNT network films with three different thicknesses were fabricated on glass substrates by the vacuum filtration and transfer methods as shown in Figure 1.

Figure 2 shows the optical and AFM images of SWCNT films fabricated by the LB and vacuum filtration method. AFM images of SWCNT LB films show that the nanotubes are highly aligned in one direction, whereas films prepared by the vacuum filtration method show random network architecture (Figure 2b). Thickness of network SWCNT films were controlled by adjusting the solution volume of the SWCNT-SHs suspension solution to 2 [Network (A)], 4 [Network (B)], and 8 mL [Network (C)], and their corresponding thicknesses were 55 ± 5, 75 ± 5, and 95 ± 5 nm, respectively (Figure 2 and Table 1). In the case of SWCNT LB film, the unidirectionally aligned structure possesses a thickness (55 ± 5 nm) similar to that of network SWCNT film (A). Optical transmittance of SWCNT films was decreased and roughness was increased as the film thickness increased, obviously due to the increase of density of nanotubes in the film (Figure S2, Supporting Information). For characterization of LB and network films, the top and cross-sectional images of these films were obtained by SEM. Density and thickness of network films showed a gradual increase with the increasing volume of SWCNT suspension (Figure 2c). In the case of SWCNT LB film, its density and thickness were similar to that of network SWCNT film (A), as indicated in Figure 2 and Table 1.

The surface wettability and surface potential of the bare glass and the SWCNT films were estimated by using a dynamic contact angle analyzer and ζ-potential measurement systems (Figure 3). As a results, the SWCNT LB and network films showed hydrophilic property (44−56°). It is also well coordinated the ζ-potential data when SWCNT film thickness was increased, the δ-potential value decreased from −48.16 to −12.38 mV, which means that our thiophenyl-modified SWCNTs has a positive potential property (ζ = 20 mV). This is a very important factor to make SWCNT-based film for

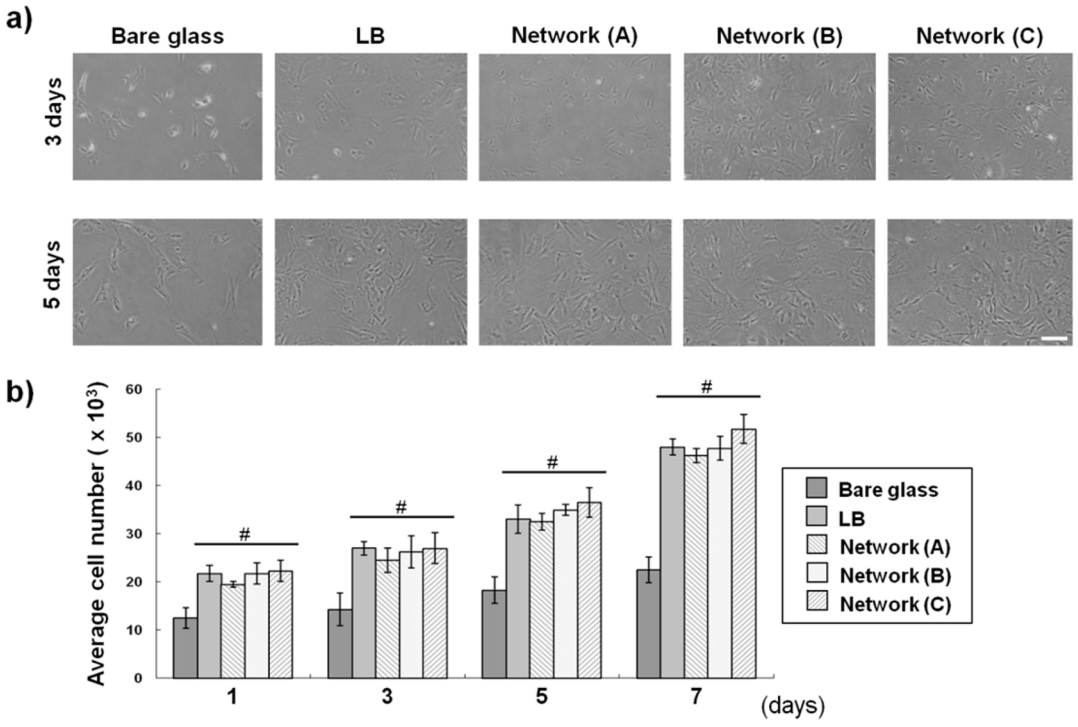

Figure 4. (a) Optical microscopic images of rMSCs cultured on a bare glass and on SWCNT films for 3 and 5 days. (b) Average cell populations on five different substrates for culture durations of 1, 3, 5, and 7 days. Scale bar, 100 μm; #, $p > 0.05$).

DOI: 10.1021/am506833q
ACS Appl. Mater. Interfaces 2015, 7, 1560−1567

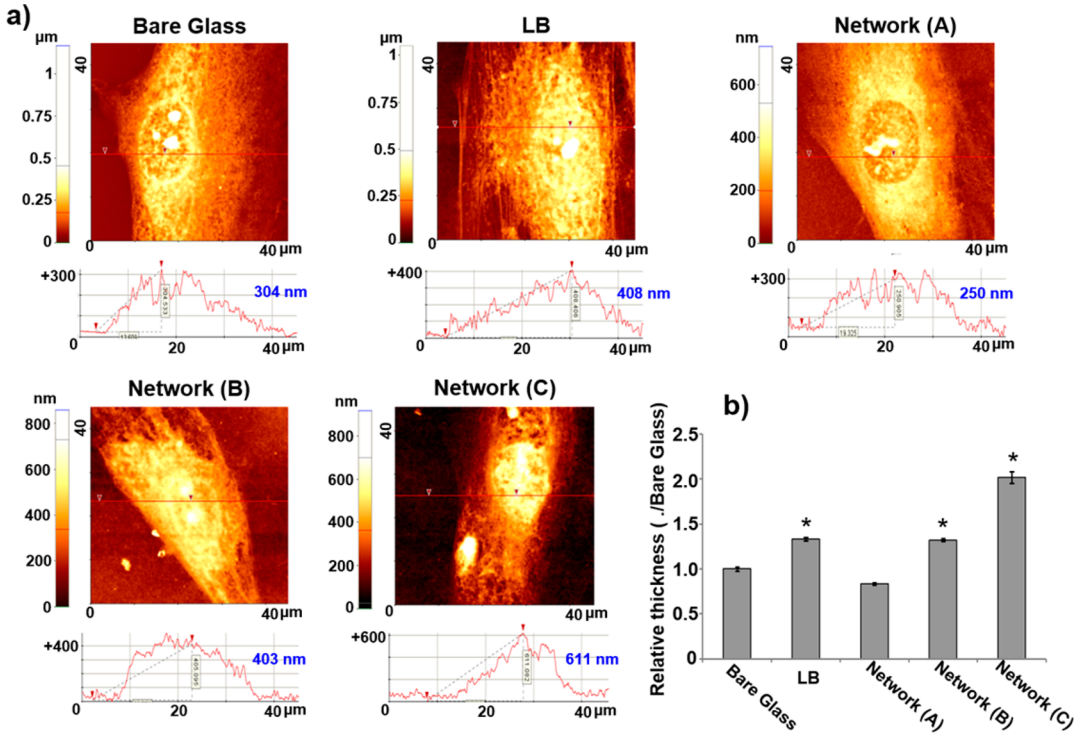

Figure 6. (a) AFM images obtained from rMSCs cultured on a glass and SWCNT films after 72 h, and (b) height profiles created from AFM images. Height profiles represent average height values of 5 cells for each sample and are analyzed using one-way analysis of variance (ANOVA). * $p < 0.05$.

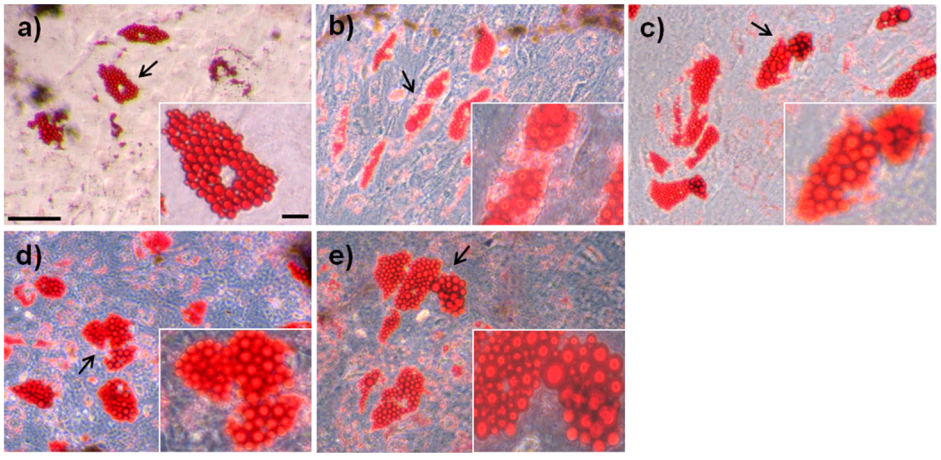

Figure 7. Evaluation of adipogenic properties of rMSCs. Cells were differentiated in TCPS (a), and (b–e) SWCNT films for 10 days, as shown by positive Oil Red O staining for adipocytes. Differentiation property was maintained in LB (b), and network (A), (B), and (C) in panels c, d, and e, respectively. Scale bar: 100 μm (for inset image, scale bar: 25 μm).

cell culture substrate because the cell membrane has a negatively charged surface, and preferentially attached on the neural or positive surface.[31]

To investigate growth pattern of rMSCs on SWCNT films with different thickness and morphology, the cells were cultured for 1, 3, 5, and 7 days, as summarized in Figure 4. For this study, rMSCs were obtained from adult Sprague-Dawley rats (Samtako, Sungnam, Korea) by the isolation method described in our previous report, and passage 4 was used in this study.[33] Optical micrographs of rMSCs, which were cultured on SWCNT LB film as well as on network films, indicate that cells appear relatively narrow in shape and do not show significant morphological changes at 3 and 5 days. On the other hand, cells cultured on a bare glass were more spread out on the surface of the substrate (Figure 4a). The shape, morphology and the growth rate of rMSCs grew on SWCNT LB and network films were similar to those cultured on a standard culture substrate of tissue culture polystyrene (TCPS) plate (data are not shown). The relative degrees of proliferation, indicated as cell population in Figure 4b, of rMSCs cultured on SWCNT LB and network films were considerably higher than those of the cells cultured on the bare glass. Although the morphologies were the same, the growth rate of rMSCs appeared to increase with increasing thickness of the SWCNT film. The following phenomenon is attributed to a large number of nanopores and high roughness of thicker SWCNT film, which provide a suitable three-dimensional culture condition for the proliferation and differentiation of

DOI: 10.1021/am506833q
ACS Appl. Mater. Interfaces 2015, 7, 1560–1567

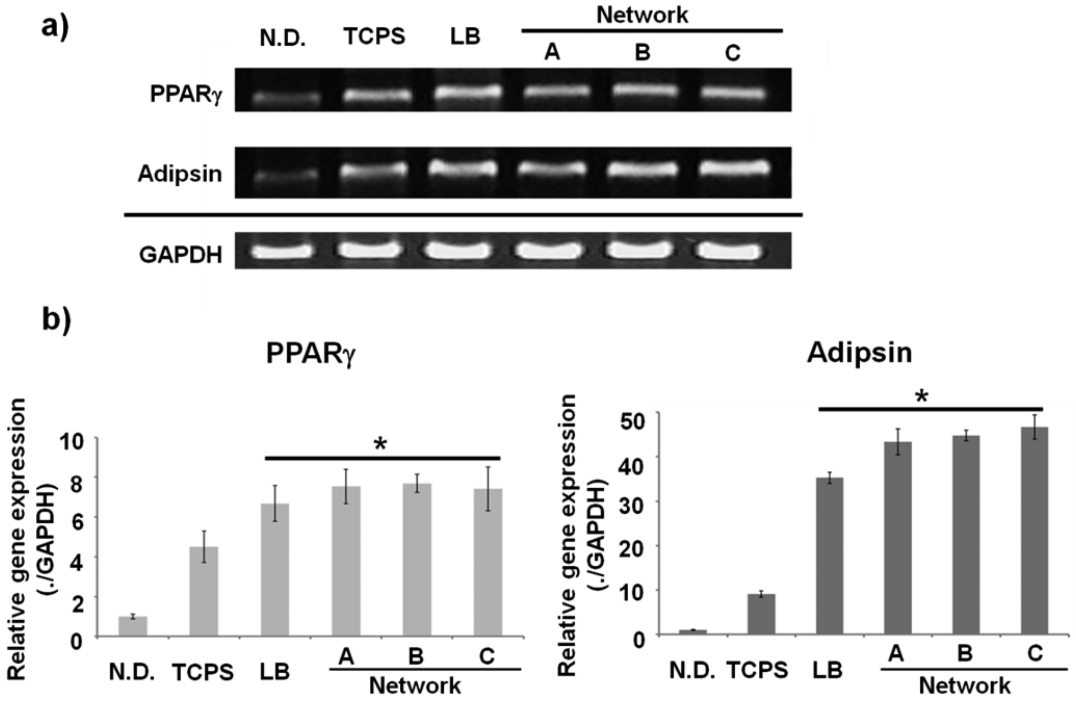

Figure 8. Analysis of gene expression with adipose-specific marker. (a) Semiquantitative RT-PCR was performed using rMSCs differentiated in TCPS and SWCNT films. (b) PPARγ and adipsin were represented with related-gene expression ratio versus glyceraldehydes 3-phosphate dehydrogenase (GAPDH) control. The gene expression level was calculated 5 times for each sample, and analyzed using one-way analysis of variance (ANOVA). * $p < 0.05$ (comparison with N.D. or TCPS); N.D., nondifferentiated control.

rMSCs. CNTs have some features common to that of natural extracellular matrix (ECM), which are essential for the scaffold formation. High degree of flexibility and elasticity are important characteristics of CNTs that facilitate the cell adhesion. Another important common feature CNT and ECM is the presence of porosity of similar diameter. The high degree of porosity found in nanotubes makes them applicable as scaffolds, since the natural ECM is highly porous and this is the fundamental factor for the tissue integration.[31]

To evaluate viability of rMSCs cultured on SWCNT LB and network films, MTT assays were performed with cells which were cultured for 72 h (Figure 5). Compared to cells grown on bare glass as a control, no significant viability change was observed for rMSCs cultured on both SWCNT LB film and network films with different thickness and roughness levels. These results indicate that the SWCNT films could be used as substrates for growth of rMSCs without any toxic effect.

Structural characteristics and morphology of the rMSCs cultured on the SWCNT films were analyzed by using high resolution SWCNT capped AFM tips.[34] Figure 6 shows the typical AFM images and thickness profiles of rMSCs cultured on different substrates. The average thickness of rMSCs was about 300 nm for cells cultured on the bare glass, whereas those cultured on SWCNT LB and network films were relatively higher and reached above 600 nm on thicker network SWCNT films. Apparently, the thickness of the cell was closely related on the thickness of SWCNT film, as shown in Figure 6b. Cells grown on SWCNT LB film were 400 nm in height, which was thicker than height of cells grown on network film at similar thickness (Network (A)). The thickness of the cells may reflect their vitality, as suggested in Figures 4 and 6. Interestingly, in the case of SWCNT LB film, cytoskeleton structures of rMSCs were grown in one direction, which was parallel to the orientation of the SWCNT bundles (Figure S3, Supporting Information). However, in the case of network films, the growth directions of cell cytoskeleton were randomized (Figures 6a and S3, Supporting Information). This result revealed that growth of the cell was closely related to the contact between the cell and SWCNT surface. In a previous study, Yourek et al. reported the changes of cytoskeletal structures of MSCs with respect to culture condition during differentiation.[35] Although mechanism for the change in cytoskeleton structure is not fully understood in the case of MSCs, it is clear that the SWCNT films with different morphology induce different contact behaviors, and consequently shape of the cultured cells varies accordingly.

Furthermore, to investigate effect of SWCNT films on differentiation property of rMSCs, adipogenesis was induced using adipogenic differentiation medium (PromoCell, Heidelberg, Germany), and the cells were stained with Oil Red O (Sigma, MO, USA). As shown in Figure 7, the differentiation property of rMSCs was maintained in SWCNT LB and network films. The differentiation efficiency of rMSCs cultured on SWCNT LB and network films was different from that of those cultured under TCPS condition. In particular, the size of lipid vesicles in rMSCs on SWCNT LB and network films was 2- to 3-fold larger than that on TCPS (Figure 7a–e, inset image).

In addition, mRNA level of peroxisome proliferator-activated receptor PPARγ and adipsin, which was known as an adipocyte specific marker, was significantly elevated in adipocytes cultured on SWCNT films (Figure 8).

These results demonstrate that SWCNT films can provide better conditions for maintenance and promote better the differentiation property of rMSCs than TCPS. We assume that they are generated from surface area of both type of SWCNT films, particularly nanoporous structure of network SWCNT films (Figure 2b). Unlike TCPS, nanopores in SWCNT films

DOI: 10.1021/am506833q
ACS Appl. Mater. Interfaces 2015, 7, 1560–1567

provide suitable three-dimensional culture condition for rMSCs proliferation and differentiation, as suggested in Figures 4 and 7. It is well-known that affinity of protein to the surface of SWCNTs is relatively higher due to effective hydrophobic interactions. Valenti et al. reported a real-time adsorption measurement of bovine serum albumin (BSA) on CNT coated surfaces by reflectometry,[36] and they demonstrated that the adsorption of BSA on the CNT is stronger than that on silica surface, because of both electrostatic and hydrophobic interactions of CNT surface with BSA molecules. According to their results, BSA molecules arriving at the CNT surface may adopt a preferred orientation with the positive and nonpolar patches of the protein facing the hydrophobic sorbent surface, resulting in an attachment-controlled adsorption process. In addition, Guo et al. reported that SWCNT caused dose-dependent adsorption and depletion of over 14 amino acids and vitamins from cell culture medium.[37] They showed that the amino acids and vitamins existing in cell culture medium exhibited higher affinity for graphitic carbon-hydrophobicity and planarity/sp^2 hybridization of $\pi-\pi$ interactions and positively charged solutes. It is also well-known that cell adhesion to ECM is usually dictated by focal adhesions (FAs), which link actin cytoskeleton to ECM and provide regions for signal transduction to regulate cell growth.[38] Similarly our results suggest that effective adsorption of growth factor proteins of the cell and nutrients in the culture media contribute promotion of cell proliferation and differentiation on SWCNT films. Therefore, the strong protein adsorption ability of SWCNT films is one of the possible reasons for enhanced proliferation and differentiation, in addition to nanoporous structures of network SWCNT films.

4. CONCLUSIONS

We have demonstrated that nanoscale variations in the thickness, roughness of the SWCNT films, and surface property of SWCNTs positively affect growth and differentiation of rMSCs. Our results show that the SWCNT films did not show any cytotoxicity to MSCs. The SWCNT network film with a thickness of 95 ± 5 nm and roughness value of 9.81 nm revealed a faster rate of growth and higher cell thickness for rMSCs. This particular condition may serve as the optimal surface and topological properties for growth of rMSCs. In addition, our adipogenesis result on the SWCNT films suggests that it can be a tool for understanding mechanism and for control of proliferation and differentiation of MSCs. Our results suggest novel prospects of MSCs for differentiation to other specific cells through precise control of surface property including thickness and morphology of SWCNT films. This study also demonstrates the possibility of utilizing SWCNT films as a culture substrate with capability of promoting growth and differentiation of MSCs.

■ ASSOCIATED CONTENT

Supporting Information

(Figure S1) Characterization of the SWCNT bundle by SEM and AFM (a) photograph of stable homogeneous solution of SWCNT-SH in $CHCl_3$ (b) SEM image and (c) AFM image of SWCNT bundles. The bundle diameter of SWCNT was measured by height profile of AFM images. (Figure S2) Transmittance spectra of bare glass and 4 different SWCNT films. (Figure S3) AFM images of rMSCs cultured on bare glass and four different SWCNT films. This material is available free of charge via the Internet at http://pubs.acs.org.

■ AUTHOR INFORMATION

Corresponding Authors

*Prof. Gwang Lee. E-mail: glee@ajou.ac.kr.
*Prof. Jae-Ho Kim. E-mail: jhkim@ajou.ac.kr.

Present Address

[§]Asian Herb Cosmetic Research Team, Amorepacific R&D center, 1920 Yonggu-daero, Giheung-gu, Yongin-Si, Gyeonggi-do, Korea 446-729.

Author Contributions

[⊥]These authors contributed equally to this work.

Notes

The authors declare no competing financial interest.

■ ACKNOWLEDGMENTS

This research was supported by Basic Science Research Program through the National Research Foundation of Korea (NRF) funded by the Ministry of Education (No. 2009-0093826). In addition, we thank the BK21 program of molecular science and technology at Ajou University.

■ ABBREVIATIONS

AFM, atomic force microscopy
CNT, carbon nanotube
DMF, dimethylformamide
LB film, Langmuir−Blodgett film
MSC, mesenchymal stem cells
MWCNT, multi-walled carbon nanotube
SEM, scanning electron microscopy
SWCNT, single-walled carbon nanotube

■ REFERENCES

(1) Alfaro, M. P.; Vincent, A.; Saraswati, S.; Thorne, C. A.; Hong, C. C.; Lee, E.; Young, P. P. sFRP2 Suppression of Bone Morphogenic Protein (BMP) and Wnt Signaling Mediates Mesenchymal Stem Cell (MSC) Self-Renewal Promoting Engraftment and Myocardial Repair. *J. Biol. Chem.* **2010**, *285*, 35645−35653.

(2) Pittenger, M. F.; Mackay, A. M.; Beck, S. C.; Jaiswal, R. K.; Douglas, R.; Mosca, J. D.; Moorman, M. A.; Simonetti, D. W.; Craig, S.; Marshak, D. R. Multilineage Potential of Adult Human Mesenchymal Stem Cells. *Science* **1999**, *284*, 143−147.

(3) Sarugaser, R.; Hanoun, L.; Keating, A.; Stanford, W. L.; Davies, J. E. Human Mesenchymal Stem Cells Self-Renew and Differentiate According to a Deterministic Hierarchy. *PLoS One* **2009**, *4*, e6498.

(4) George, J.; Kuboki, Y.; Miyata, T. Differentiation of Mesenchymal Stem Cells into Osteoblasts on Honeycomb Collagen Scaffolds. *Biotechnol. Bioeng.* **2006**, *95*, 404−411.

(5) Mackay, A. M.; Beck, S. C.; Murphy, J. M.; Barry, F. P.; Chichester, C. O.; Pittenger, M. F. Chondrogenic Differentiation of Cultured Human Mesenchymal Stem Cells from Marrow. *Tissue Eng.* **1998**, *4*, 415−428.

(6) Sekiya, I.; Larson, B. L.; Vuoristo, J. T.; Cui, J. G.; Prockop, D. J. Adipogenic Differentiation of Human Adult Stem Cells from Bone Marrow Stroma (MSCs). *J. Bone. Miner. Res.* **2004**, *19*, 256−264.

(7) Woodbury, D.; Schwarz, E. J.; Prockop, D. J.; Black, I. B. Adult Rat and Human Bone Marrow Stromal Cells Differentiate into Neurons. *J. Neurosci. Res.* **2000**, *61*, 364−370.

(8) Friedenstein, A. J.; Deriglasova, U. F.; Kulagina, N. N.; Panasuk, A. F.; Rudakowa, S. F.; Luria, E. A.; Ruadkow, I. A. Precursors for Fibroblasts in Different Populations of Hematopoietic Dells As Detected by the in Vitro Colony Assay Method. *Exp. Hematol. (N. Y., NY, U. S.)* **1974**, *2*, 83−92.

(9) Zuk, P. A.; Zhu, M.; Ashjian, P.; Ugarte, D. A.; De Huang, J. I.; Mizuno, H.; Alfonso, Z. C.; Fraser, J. K.; Benhaim, P.; Hedrick, M. H. Human Adipose Tissue Is a Source of Multipotent Stem Cells. *Mol. Biol. Cell* **2002**, *13*, 4279−4295.

DOI: 10.1021/am506833q
ACS Appl. Mater. Interfaces 2015, 7, 1560−1567

(10) Ko, E.; Lee, K. Y.; Hwang, D. S. Human Umbilical Cord Blood-Derived Mesenchymal Stem Cells Undergo Cellular Senescence in Response to Oxidative Stress. *Stem Cells Dev.* **2012**, *21*, 1877−1886.
(11) Ballas, C. B.; Zielske, S. P.; Gerson, S. L. Adult Bone Marrow Stem Cells for Cell and Gene Therapies: Implications for Greater Use. *J. Cell Biochem. Suppl.* **2002**, *38*, 20−28.
(12) Iijima, S. Helical Microtubules of Graphitic Carbon. *Nature* **1991**, *354*, 56−58.
(13) Bhattacharya, M.; Wutticharoenmongkol-Thitiwongsawet, P.; Hamamoto, D. T.; Lee, D.; Cui, T.; Prasad, H. S.; Ahmad, M. Bone Formation on Carbon Nanotube Composite. *J. Biomed. Mater. Res., Part A* **2011**, *96*, 75−82.
(14) Benincasa, M.; Pacor, S.; Wu, W.; Prato, M.; Bianco, A.; Gennaro, R. Antifungal Activity of Amphotericin B Conjugated to Carbon Nanotubes. *ACS Nano* **2010**, *5*, 199−208.
(15) Gul, H.; Lu, W.; Xu, P.; Xing, J.; Chen, J. Magnetic Carbon Nanotube Labelling for Haematopoietic Stem/Progenitor Cell Tracking. *Nanotechnology* **2010**, *21*, 155101.
(16) Nho, Y.; Kim, J. Y.; Khang, D.; Webster, T. J.; Lee, J. E. Adsorption of Mesenchymal Stem Cells and Cortical Neural Stem Cells on Carbon Nanotube/Polycarbonate Urethane. *Nanomedicine (London, U. K.)* **2010**, *5*, 409−417.
(17) Keefer, E. W.; Botterman, B. R.; Romero, M. I.; Rossi, A. F.; Gros, G. W. Carbon Nanotube Coating Improves Neuronal Recordings. *Nat. Nanotechnol.* **2008**, *3*, 434−439.
(18) Cellot, G.; Cilia, E.; Cipollone, S.; Rancic, V.; Sucapane, A.; Giordani, S.; Gambazzi, L.; Markram, H.; Grandolfo, M.; Scaini, D.; Gelain, F.; Casalis, L.; Prato, M.; Giugliano, M.; Ballerini, L. Carbon Nanotubes Might Improve Neuronal Performance by Favouring Electrical Shortcuts. *Nat. Nanotechnol.* **2009**, *4*, 126−133.
(19) Cai, D.; Blair, D.; Dufort, F. J.; Gumina, M. R.; Huang, Z.; Hong, G.; Wagner, D.; Canahan, D.; Kempa, K.; Ren, Z. F.; Chiles, T. C. Interaction between Carbon Nanotubes and Mammalian Cells: Characterization by Flow Cytometry and Application. *Nanotechnology* **2008**, *19*, 345102.
(20) Porter, A. E.; Gass, M.; Bendall, J. S.; Muller, K.; Goode, A.; Skepper, J. N.; Midgley, P. A.; Welland, M. Uptake of Noncytotoxic Acid-Treated Single-Walled Carbon Nanotubes into the Cytoplasm of Human Macrophage Cells. *ACS Nano* **2009**, *3*, 1485−1492.
(21) Kim, J. S.; Song, K. S.; Joo, H. J.; Lee, J. H.; Yu, J. I. Determination of Cytotoxicity Attributed to Multiwall Carbon Nanotubes (MWCNT) in Normal Human Embryonic Lung Cell (WI-38) Line. *J. Toxicol. Environ. Health, Part A* **2010**, *73*, 1521−1529.
(22) Mooney, E.; Dockery, P.; Greiser, U.; Murphy, M.; Barron, V. Carbon Nanotubes and Mesenchymal Stem Cells: Biocompatibility, Proliferation and Differentiation. *Nano Lett.* **2008**, *8*, 2137−2143.
(23) Jan, E.; Kotov, N. A. Successful Differentiation of Mouse Neural Stem Cells on Layer-by-Layer Assembled Single-Walled Carbon Nanotube Composite. *Nano Lett.* **2007**, *7*, 1123−1128.
(24) Tay, G. H.; Gu, H.; Leong, W. S.; Yu, H.; Li, H. Q.; Heng, B. C.; Tantang, H.; Loo, S. C. J.; Li, L. J.; Tan, L. P. Cellular Behavior of Human Mesenchymal Stem Cells Cultured on Single-Walled Carbon Nanotube Film. *Carbon* **2010**, *48*, 1095−1104.
(25) Mazzatenta, A.; Giugliano, M.; Campidelli, S.; Gambazzi, L.; Businaro, L.; Markram, H.; Prato, M.; Ballerini, L. Interfacing Neurons with Carbon Nanotubes: Electrical Signal Transfer and Synaptic Stimulation in Cultured Brain Circuits. *J. Neurosci.* **2007**, *27*, 6931−6936.
(26) Malarkey, E. B.; Fisher, K. A.; Bekyarova, E.; Liu, W.; Haddon, R. C.; Parpura, V. Conductive Single-Walled Carbon Nanotube Substrates Modulate Neuronal Growth. *Nano Lett.* **2009**, *9*, 264−268.
(27) Park, S. Y.; Choi, D. S.; Jin, H. J.; Park, J.; Byun, K.-E.; Lee, K.-B.; Hong, S. Polarization-Controlled Differentiation of Human Neural Stem Cells Using Synergistic Cues from the Patterns of Carbon Nanotube Monolayer Coating. *ACS Nano* **2011**, *5*, 4704−4711.
(28) Mattson, M. P.; Haddon, R. C.; Rao, A. M. Molecular Functionalization of Carbon Nanotubes and Use as Substrates for Neuronal Growth. *J. Mol. Neurosci.* **2000**, *14*, 175−182.
(29) Firkowska, I.; Godehardt, E.; Giersing, M. Interaction between Human Osteoblast Cells and Inorganic Two-Dimensional Scaffolds Based on Multiwalled Carbon Nanotubes: A Quantitative AFM Study. *Adv. Funct. Mater.* **2008**, *18*, 3765−3711.
(30) Kotov, N. A.; Winter, J. O.; Clements, I. P.; Jan, E.; Timko, B. P.; Campidelli, S.; Pathak, S.; Mazzatenta, A.; Lieber, C. M.; Prato, M.; Bellamkonda, R. V.; Silva, G. A.; Kam, N. W. S.; Patolsky, F.; Ballerini, L. Nanomaterials for Neural Interfaces. *Adv. Mater.* **2009**, *21*, 3970−4004.
(31) Tonelli, F. M. P.; Santos, A. K.; Gomes, K. N.; Lorencon, E.; Guatimosim, S.; Ladeira, L. O.; Resende, R. R. Carbon Nanotube Interaction with Extracellular Matrix Proteins Producing Scaffolds for Tissue Engineering. *Int. J. Nanomed.* **2012**, *7*, 4511−4529.
(32) Choi, S. W.; Kang, W. S.; Lee, J. H.; Najeeb, C. K.; Chun, H. S.; Kim, J. H. Patterning of Hierarchically Aligned Single-Walled Carbon Nanotube Langmuir-Blodgett Films by Microcontact Printing. *Langmuir* **2010**, *26*, 15680−1568.
(33) Yoon, J. K.; Park, B. N.; Shim, W. Y.; Shin, J. Y.; Lee, G.; Ahn, Y. H. In Vivo Tracking of 111In-Labeled Bone Marrow Mesenchymal Stem Cells in Acute Brain Trauma Model. *Nucl. Med. Biol.* **2010**, *37*, 381−388.
(34) Lee, J. H.; Kang, W. S.; Choi, B. S.; Choi, S. W.; Kim, J. H. Fabrication of Carbon Nanotube AFM Probes using the Langmuir-Blodgett Technique. *Ultramicroscopy* **2008**, *108*, 1163−1167.
(35) Yourek, G.; Hussain, M. A.; Mao, J. J. Cytoskeletal Changes of Mesenchymal Stem Cells during Differentiation. *ASAIO J.* **2007**, *53*, 219−288.
(36) Valenti, L. E.; Fiorito, P. A.; García, C. D.; Giacomelli, C. E. The Adsorption-Desorption Process of Bovine Serum Albumin on Carbon Nanotubes. *J. Colloid Interface Sci.* **2007**, *307*, 349−356.
(37) Guo, L.; Bussche, A. V. D.; Buechner, M.; Yan, A.; Kane, A. B.; Hurt, R. H. Adsorption of Essential Micronutrients by Carbon Nanotubes and the Implications for Nanotoxicity Testing. *Small* **2008**, *4*, 721−727.
(38) Namgung, S.; Kim, T.; Baik, K. Y.; Lee, M.; Nam, J. M.; Hong, S. Fibronectin-Carbon-Nanotube Hybrid Nanostructures for Controlled Cell Growth. *Small* **2011**, *7*, 56−61.

DOI: 10.1021/am506833q
ACS Appl. Mater. Interfaces 2015, 7, 1560−1567